J Sol-Gel Sci Technol (2014) 69:33–39
DOI 10.1007/s10971-013-3181-8

ORIGINAL PAPER

Selective oxidation of styrene efficiently catalyzed by spinel Mg–Cu ferrite complex oxides in water

Xiaodong Cai · Haiyan Wang · Qianping Zhang · Jinhui Tong

Received: 18 June 2013 / Accepted: 8 October 2013 / Published online: 18 October 2013

Abstract Magnetic ferrite $Mg_{1-x}Cu_xFe_2O_4$ (x = 0, 0.1, 0.3, 0.5, 0.7, 0.9, 1.0) nanocrystalline complex oxides were prepared by sol–gel auto-combustion method, and characterized by X-ray diffractometry, Fourier transform infrared spectrophotometry, Raman spectrometry, scanning electron microscopy and transmission electron microscopy. Their catalytic performances were evaluated in oxidation of styrene in water using hydrogen peroxide (30 %) as oxidant. The samples were found to be efficient catalysts for the oxidation of styrene to benzaldehyde. Especially, when $Mg_{0.5}Cu_{0.5}Fe_2O_4$ was used as catalyst, 21.8 % of styrene conversion and 83.9 % of selectivity for benzaldehyde were obtained at 80 °C for 9 h reaction. The catalyst can be magnetically separated easily for reuse and no obvious loss of activity was observed when reused in five consecutive runs.

Keywords Sol–gel auto-combustion · Magnetic nanocrystals · $Mg_xCu_{1-x}Fe_2O_4$ complex oxide · Styrene oxidation · Hydrogen peroxide

1 Introduction

Catalytic oxidation of styrene is of great interest because styrene oxide and benzaldehyde are important and versatile synthetic intermediates in chemical industry [1]. Especially, benzaldehyde is a very important fine chemical product and can be widely used in many fields, such as medicine, dyes, flavors and resin additives. It is also a very important intermediate in synthesis of other aroma compounds [2, 3]. Great efforts have been made to develop novel catalytic systems for oxidation of styrene in the past years [4–7]. Among the reported systems, heterogeneous ones using green oxidants and solvents are particularly desirable in both economical and environmental aspects [8, 9]. Metal oxides, especially magnetic nanocrystals of complex oxides such as spinel ferrites become more important in recent years due to both their unique properties and broad range of applications in diverse areas such as magnetic recording and separation, ferrofluid, magnetic resonance imaging (MRI), biomedicine, catalysts, gas sensors, high quality ceramics and superparamagnetic materials [10–13]. A great advantage of using magnetic ferrite nanocrystals as catalysts in liquid-phase reactions is that the catalysts are not only thermally and chemically stable in the solution medium, but also easy to be recovered because of their magnetic property. As a matter of fact, these catalysts can be separated from the reaction medium by simply placing a magnetic field on the surface of the flask. Many examples for catalytic oxidation of styrene using spinel ferrites as catalysts were reported, such as $MgFe_2O_4$ [14], $SrFe_2O_4$ [15], $CaFe_2O_4$ [16], nickel and zinc ferrites [17]. Ni–Gd ferrites [18] and ferrites supported silver [19]. However, most of these oxidation reactions have been carried out in organic solvents with low efficiency.

The properties of ferrites are highly related to their shapes, sizes and structures, which can be adjusted through the synthesizing processes. Significant number of methods have been developed to prepare the ferrite nanomaterials with various properties, for instance, sonochemical reactions [20, 21], mechanochemical synthesis [22, 23],

X. Cai · H. Wang · Q. Zhang · J. Tong
Key Laboratory of Eco-Environment-Related Polymer Materials, Ministry of Education, Lanzhou, People's Republic of China

X. Cai · H. Wang · Q. Zhang · J. Tong (✉)
Key Laboratory of Gansu Polymer Materials, College of Chemistry and Chemical Engineering, Northwest Normal University, Lanzhou 730070, People's Republic of China
e-mail: jinhuitong@126.com

hydrolysis of precursors [24], flow injection synthesis [25], aqueous co-precipitation [26], hydrothermal method [27] and sol–gel auto-combustion method [28]. Among these techniques, sol–gel auto-combustion synthesis has been proved to be a simple and economical way to prepare nanopowders [28, 29]. Combining the advantages of chemical sol–gel and combustion processes, sol–gel auto-combustion synthesis gives rise to a thermally induced anionic redox reaction. The energy released from the reaction between oxidant and reductant is adequate to form a desirable phase within very short time. The process exhibits the advantages of inexpensive precursors, a simple preparation process, and can produce highly reactive nano-sized powder [30].

In our previous work [31], $CoFe_2O_4$ nanocrystal synthesized by sol–gel auto-combustion method was proved to be highly active and easily recovered catalyst for the oxidation of cyclohexane by molecular oxygen without addition of solvents or reductants. As part of our interest in hydrocarbon oxidation catalyzed by spinel ferrites, we are reporting here Mg–Cu spinel ferrites synthesized by sol–gel auto-combustion method can efficiently catalyze the oxidation of styrene to produce benzaldehyde in water using hydroperoxide as green oxidant.

2 Experimental

2.1 Materials and equipments

All reagents are of analytical grade and were used as received. FT-IR spectra were measured on a Nexus 870 FT-IR spectrophotometer by diffused reflectance accessory in the 4,000–400 cm^{-1} range. XRD patterns of the samples were collected using a PANalytical X'Pert Pro diffractometer with Cu Kα radiation in the 2θ range of 10°–80° with a scanning rate of 5°/min and a voltage and current of 40 kV and 30 mA. Visible Raman spectra were recorded on a Jobin–Yvon U1000 scanning double monochromator in the range of 300–1,000 cm^{-1} with a spectral resolution of 4 cm^{-1}. The line at 532 nm from a DPSS 532 Model 200 532 nm single-frequency laser was used as the excitation source. SEM and TEM micrographs were obtained using a JSM-5600LV and Hitachi H-600 microscope using 10 and 120 kV acceleration voltages respectively. The oxidation products were determined by an HP 6890/5973 GC/MS instrument and quantified by a Shimadzu GC-2010 gas chromatograph.

2.2 Synthesis of the catalysts

The spinel Mg–Cu ferrite catalysts $Mg_{1-x}Cu_xFe_2O_4$ (x = 0, 0.1, 0.3, 0.5, 0.7, 0.9, 1) were prepared by the sol–gel auto-combustion route under optimized conditions reported in our previous work [32]. In a typical procedure, stoichiometric amounts of $Mg(NO_3)_2{\cdot}6H_2O$, $Cu(NO_3)_2{\cdot}3H_2O$, $Fe(NO_3)_3{\cdot}9H_2O$ and citric acid were completely dissolved in distilled water with 1:1 molar ratio of metals to citric acid and 0.1 mol L^{-1} of metals concentration. Concentrated ammonia (25–28 %) was added slowly under constant stir to adjust the solution to neutral. The solution was evaporated in an oil bath at 80 °C under continuous stirring until a brown gel formed. After the reaction, the formed gel was dried at 120 °C until a spumous xerogel was obtained. Then the produced xerogel was ignited at 650 °C, a self-propagating combustion process occurred and an olive brown product was obtained after it combusted completely. Seven samples with different ratios of Mg to Cu were prepared as described above and designated as **cat.1–7**, respectively. The samples were ground finely and then used to catalyze the oxidation of styrene with hydrogen peroxide.

2.3 Oxidation of styrene

The selective oxidation of styrene was carried out in a 25 mL round bottom flask equipped with a Teflon coated magnetic stirrer and a reflux condenser. In a typical procedure, 10 mg of catalyst, 2 mL (17.4 mmol) of styrene, 5 mL of water and 4.5 mL of hydrogen peroxide (30 %), molar ratio of styrene/H_2O_2 = 2:5, were added successively into the flask. The flask is then immersed in an oil bath at desired temperature and time with stirring. The products were identified by GC–MS and quantified by GC using toluene as internal standard.

3 Results and discussion

3.1 Characterization of catalysts

The XRD patterns of the samples **cat.1–6** confirm existing of crystalline spinel (Fig. 1). The seven peaks at 18.3, 30.2, 35.4, 43.2, 53.1, 57.2 and 62.7° can be ascribed to the reflection of (111), (220), (311), (400), (422), (511) and (440) diffractions of $MgFe_2O_4$ (JCPDS NO. 88-1936) and $CuFe_2O_4$ (JCPDS NO. 77-0010) spinels. The XRD pattern of the sample **cat.7** is in agreement with the standard one for body-centered tetragonal $CuFe_2O_4$, the diffraction peaks at 2θ values of 18.3°, 29.8°, 34.6°, 35.9°, 37.1°, 41.6°, 43.8°, 58.0°, 62.0°, 63.8° and 74.7° can be ascribed to the reflection of (101), (112), (103), (211), (202), (004), (220), (321), (224), (400) and (413) diffractions of the $CuFe_2O_4$ (JCPDS NO. 34-0425), respectively (Fig. 1). The mean particle sizes of the samples based on the Sherrer equation are 28, 20, 22, 27, 23, 18 and 26 nm for **cat.1–7**, respectively.

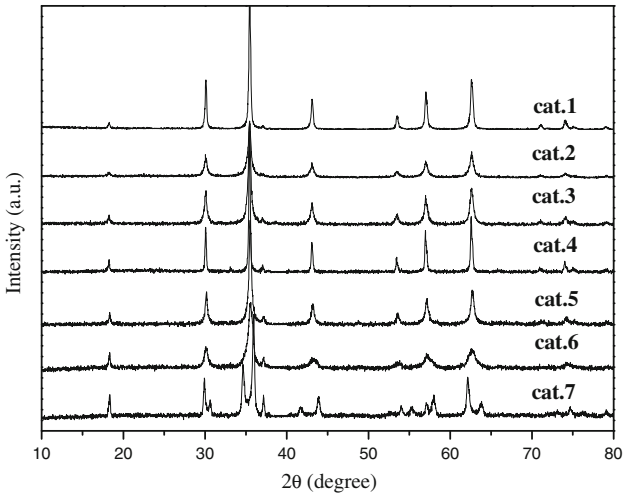

Fig. 1 The XRD patterns of the samples **cats. 1–7**

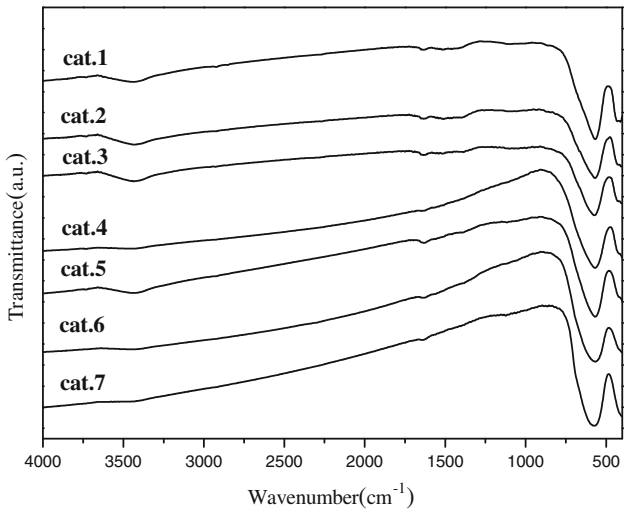

Fig. 2 The FT-IR spectra of **cats. 1–7**

Figure 2 shows the FT-IR spectra of the seven samples. A strong band at around 570 cm^{-1} for **cat.1–7** is presented. It is associated with the Fe–O stretching vibrations in magnesium ferrite and copper ferrite phase [33]. Two weak absorption bands around 3,420 and 1,630 cm^{-1} can be attributed to stretching and bending vibrations of O–H in adsorbed water. No characteristic bands corresponding to citric acid or NO^{3-} appeared, and this indicates that no citric acid or NO^{3-} is residual in the samples.

The Raman spectra of the samples are shown in Fig. 3. The low-frequency vibrations (below 600 cm^{-1}) are attributed to motion of oxygen around the octahedral lattice sites whereas the higher frequencies are attributed to oxygen around tetrahedral sites [34]. Thus, the intense band in the Raman spectra of the samples at 696 cm^{-1} can be assigned to the A_{1g} symmetry (tetrahedral) [35], and the 479 cm^{-1} band is characteristic of the octahedral sites [36].

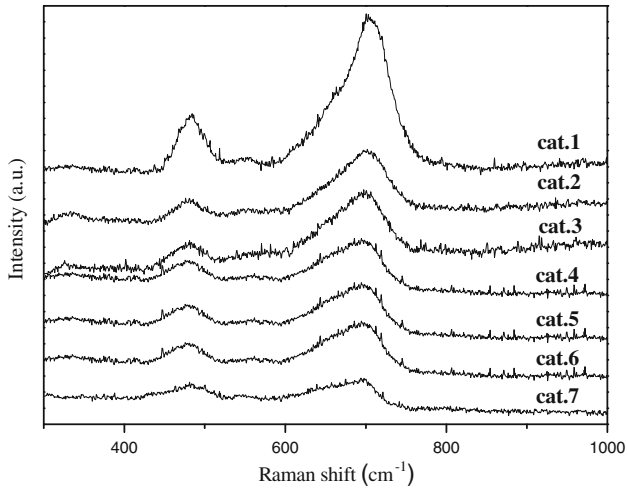

Fig. 3 The Raman spectra of **cats. 1–7**

The morphologies of the samples were also characterized by SEM and TEM. The SEM and TEM images of **cat.4** are shown in Fig. 4 as representations. The sample **cat.4** features nanoparticles with an irregular morphology and a broad particle size distribution ranging from 10–20 to 30–50 nm, with a high percentage of small particles (25–30 nm). It is clear that the sample have particle agglomeration forms. Other samples showed similar morphologies with **cat.4** except for different particle sizes as calculated from the Sherrer equation based on the XRD patterns.

3.2 Catalysis tests

The results of styrene oxidation over the as-prepared samples **cat.1–7** are listed in Table 1. In order to check the role of the composite ferrites towards selective oxidation of styrene, a blank reaction was carried out under the same conditions. As shown in Table 1, in the absence of catalyst, almost no reaction took place as seen from GC/MS analysis (entry 1). The samples **cat.1–7** can efficiently catalyze the oxidation of styrene and benzaldehyde was found to be the major product in all cases. As expected, composite oxides of Mg–Cu ferrites showed better performances than pure one of either $MgFe_2O_4$ (entry 2) or $CuFe_2O_4$ (entry 8). Especially, $Mg_{0.5}Cu_{0.5}Fe_2O_4$ (**cat.4**) has obtained the highest styrene conversion of 16.7 % with 86.3 % of selectivity for benzaldehyde. A free radical mechanism may be involved in selective oxidation of styrene over ferrite catalysts [15]. As a fact, when the same reaction was carried out in the presence of tertiary butyl alcohol as a scavenger, only 9.2 % of styrene conversion was obtained (entry 9). It has been noted that the catalytic effectiveness of such system is due to the ability of metallic ions to migrate between the sub-lattices [14, 20, 21]. So before

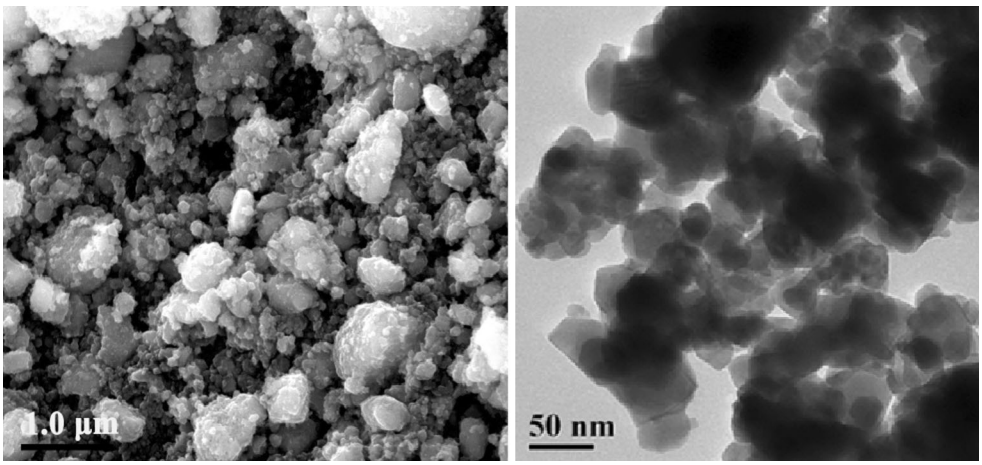

Fig. 4 The SEM and TEM images of the **cats. 4**

Table 1 Oxidation of styrene over different catalysts

Entry	Catalyst	Conversion (%)	Selectivity (%)			
			BzA	PhAA	SO	Others
1	Blank	–	–	–	–	–
2	**cat.1**	4.4	76.1	8.5	9.3	6.2
3	**cat.2**	7.3	87.7	3.7	4.9	3.6
4	**cat.3**	13.4	88.2	3.3	3.1	5.4
5	**cat.4**	16.7	86.3	3.7	3.5	6.5
6	**cat.5**	12.3	89.2	3.2	3.7	3.9
7	**cat.6**	8.6	89.2	3.5	3.2	4.1
8	**cat.7**	6.2	89.5	2.7	3.4	4.2
9	**cat.4**[a]	9.2	79.8	7.4	7.8	5.0

Reaction conditions: styrene 17.4 mmol, catalyst 10 mg, H_2O 5 mL, molar ratio of styrene:H_2O_2 2:5, temperature 70 °C, reaction time 9 h

BzA benzaldehyde, *PhAA* phenylacetaldehyde, *SO* Styrene oxide

[a] Reaction was carried out with the addition of tert-Butyl alcohol (3 wt% of styrene)

discovery of new evidences, it is reasonable to believe that appropriate molar ratio of Mg^{II}–Cu^{II} in **cat.4** is in favor of migration of metallic ions between the sub-lattices consequently. This possibility maybe account for optimum catalytic activity of $Mg_{0.5}Cu_{0.5}Fe_2O_4$ (**cat.4**). In order to optimize the reaction conditions, the sample $Mg_{0.5}Cu_{0.5}Fe_2O_4$ was chosen as catalyst to optimize the reaction conditions and investigate the recyclable performance of the catalysts.

3.3 Effect of the solvents

Table 2 shows effects of different solvents on styrene conversion and products distribution over $Mg_{0.5}Cu_{0.5}Fe_2O_4$. It is clear that aprotic solvents like acetonitrile and acetone are more favorable for the conversion of styrene while protic ones are more favorable for formation of benzaldehyde, Which is consistent with the reported results on $Mg_xFe_{3-x}O_4$ and AFe_2O_4(A = Fe, Ni, Zn) catalysts [14, 17]. As a result, the highest styrene conversion of 40.5 % and benzaldehyde selectivity of 86.3 % were obtained in acetonitrile and water, respectively. The $Mg_{0.5}Cu_{0.5}Fe_2O_4$ showed much higher efficiency than analogous catalysts reported (entry 5 and 6) and much higher turnover number can be obtained in less reaction time. Although acetonitrile is most favorable for styrene conversion, water is selected as the most environmentally friendly solvent for following investigations in pursuit of higher benzaldehyde selectivity.

3.4 Effect of styrene/H_2O_2 molar ratio

The reaction was carried out in the presence of different styrene/H_2O_2 molar ratios such as 2:1, 1:1, 2:3, 1:2 and 2:5, for which 10 mg of catalyst were taken in 5 mL of water at 70 °C for 9 h reaction. The results were listed in Table 3. It can be seen clearly that, as the molar ratio of H_2O_2 to styrene increases, styrene conversion also increases. As a result, when H_2O_2 concentration increased from 2:1 to 2:5, styrene conversion increased from 7.4 to 16.7 %. In respect of the products distribution, the selectivity for benzaldehyde varied in the range of 85.2–88.5 %, the selectivity for either phenylacetaldehyde or styrene oxide showed a little decrease, while the selectivity for other by-products increased. Considering conversion of styrene and selectivity for benzaldehyde, 2:5 was selected as the optimum molar ratio of styrene to H_2O_2.

3.5 Effect of reaction temperature

Keeping styrene:H_2O_2 with molar ratio of 2:5, the influence of reaction temperature on styrene oxidation was

Table 2 The effect of styrene oxidation with different solvents

Entry	Solvent	Conversion (%)	TON[a]	Selectivity (%)			
				BzA	PhAA	SO	Other
1	Water	16.7	64	86.3	3.7	3.5	6.5
2	Acetonitrile	40.5	155	83.8	10.7	2.9	2.6
3	Acetone	35.2	135	84.1	7.0	4.9	4.1
4	Ethanol	29.4	113	85.1	6.8	4.6	3.5
5	Acetone[b]	40.6	4	66.7	3.9	5.9	23.6
6	Acetone[c]	30.7	7	52.1	42.0		

Reaction conditions: styrene 17.4 mmol; **cat.4** 10 mg; solvent 5.0 mL; molar ratio of styrene:H_2O_2 2:5; temperature 70 °C; reaction time 9 h

BzA benzaldehyde, *PhAA* phenylacetaldehyde, *SO* styrene oxide

[a] TON = moles of substrates converted per mol of catalyst

[b] Results from Ref. [14]. Reaction conditions: styrene 10 mmol, acetone 10 mL, $Mg_{0.4}Fe_{2.6}O_4$ 100 mg, molar ratio of styrene:H_2O_2 1:1, 50 °C, 24 h

[c] Results from Ref. [17]. Reaction conditions: styrene 10 mmol, acetone 10 mL, $Ni_{0.5}Zn_{0.5}Fe_2O_4$ 100 mg, molar ratio of styrene:H_2O_2 1:1, 60 °C, 12 h, N_2 atmosphere

Table 3 The effect of styrene oxidation with different styrene/H_2O_2 molar ratio

Entry	Styrene:H_2O_2	Conversion (%)	Selectivity (%)			
			BzA	PhAA	SO	Others
1	2:1	7.4	86.1	5.5	4.4	3.9
2	1:1	9.4	87.9	4.7	3.5	3.8
3	2:3	11.5	85.2	4.6	3.8	6.4
4	1:2	13.1	88.5	3.4	3.0	5.1
5	2:5	16.7	86.3	3.7	3.5	6.5

Reaction conditions: styrene 17.4 mmol; **cat.4** 10 mg; H_2O 5 mL; temperature 70 °C; reaction time 9 h

BzA benzaldehyde, *PhAA* phenylacetaldehyde, *SO* styrene oxide

Table 4 The effect of styrene oxidation under different reaction temperature

Entry	Temperature (°C)	Conversion (%)	Selectivity (%)			
			BzA	PhAA	SO	Others
1	50	4.5	72.9	14.5	5.3	7.3
2	60	7.2	74.4	13.1	5.7	6.8
3	70	16.7	86.3	3.7	3.5	6.5
4	80	21.8	83.9	5.4	2.5	8.1
5	90	22.3	82.1	5.6	3.2	9.2

Reaction conditions: styrene 17.4 mmol; **cat.4** 10 mg; H_2O 5 mL; reaction time 9 h; molar ratio of styrene:H_2O_2 2:5

BzA benzaldehyde, *PhAA* phenylacetaldehyde, *SO* styrene oxide

evaluated in the range of 50–90 °C for 9 h reaction, and the results were listed in Table 4. It can be found that high temperature is in favor of styrene conversion. As a result, when temperature was improved from 50 to 90 °C, styrene conversion increased from 4.5 to 22.3 %. As for products distribution, with increase of temperature, selectivity for benzaldehyde increased at first and then decreased slightly, the highest value of 86.3 % was obtained at 70 °C. The selectivities for phenylacetaldehyde and styrene oxide showed a tendency of decrease with the increase of the temperature while total selectivity for other by-products increased a little. This indicates that more deeply oxidized products have formed at higher temperature.

3.6 Effect of reaction time

The influence of reaction time on styrene oxidation was investigated at 80 °C in the range of 0.5–9 h with styrene:H_2O_2 molar ratio of 2:5. As shown in Table 5, styrene conversion increased expectedly when reaction time was prolonged. In the first 2 hours, only about 5.6 % conversion was obtained. As the reaction time was increased from 3 to 8 h,the conversion of styrene increased from 5.6 to 21.2 %. The selectivity for benzaldehyde increased at first and then dropped when reaction time was over 6 h, the highest value of 87.6 % was obtained for 6 h reaction; the selectivity for phenylacetaldehyde hardly changed within the first 3 h and then dropped rapidly from 10.9 to 2.9 % when reaction time increased from 4 to 8 h; the selectivity for styrene oxide showed a tendency of decrease while the selectivity for total by-products dropped slowly in the first 5 h, but then increased greatly from 1.8 to 15.3 % when reaction time was prolonged from 6 to 8 h. In pursuit of higher selectivity for main product benzaldehyde, 6 h was selected as optimum reaction time.

3.7 Effect of catalyst amount

The effect of catalyst amount on styrene oxidation was investigated in the range of 5–20 mg at 80 °C for 6 h reaction with styrene:H_2O_2 molar ratio of 2:5. The results

Table 5 The effect of styrene oxidation with different reaction time

Entry	Time (h)	Conversion (%)	Selectivity (%)			
			BzA	PhAA	SO	Others
1	0.5	4.3	70.7	11.7	8.6	8.9
2	1	5.3	71.8	11.4	7.1	9.8
3	2	5.6	73.2	11.8	6.1	8.9
4	3	8.6	76.9	11.7	4.4	5.8
5	4	11.5	78.2	10.9	5.4	6.8
6	5	14.1	84.4	6.7	3.7	5.3
7	6	17.2	87.6	4.7	5.8	1.8
8	7	19.1	81.4	2.6	4.2	11.5
9	8	21.2	77.4	2.9	3.5	15.3

Reaction conditions: styrene 17.4 mmol; **cat.4** 10 mg; H_2O 5 mL; temperature 80 °C; styrene:H_2O_2 molar ratio 2:5

BzA benzaldehyde, *PhAA* phenylacetaldehyde, *SO* styrene oxide

Table 6 The effect of styrene oxidation with different catalyst amounts

Entry	Amount of the catalyst (mg)	Conversion (%)	Selectivity (%)			
			BzA	PhAA	SO	Others
1	5	14.0	76.9	11.1	5.5	6.5
2	10	17.2	87.6	4.7	5.8	1.8
3	15	13.9	83.9	6.7	3.2	6.1
4	20	12.6	76.6	10.3	4.9	8.2

Reaction conditions: styrene 17.4 mmol; H_2O 5 mL; temperature 80 °C; reaction time 6 h; styrene:H_2O_2 molar ratio 2:5

BzA benzaldehyde, *PhAA* phenylacetaldehyde, *SO* styrene oxide

were shown in Table 6. With increase of the catalyst amount, the styrene conversion and benzaldehyde selectivity showed similar profile, that is, increased firstly and then decreased. The highest value of 17.2 % for styrene conversion was obtained when 10 mg catalyst was used. However, with further increase of catalyst amount to 20 mg, styrene conversion decreased to 12.6 % possibly due to adsorption or chemisorptions of two reactants on separate catalyst particles, thereby reducing the chance to interact. Similar observations were noted by Sharma and Pardeshi [9, 15]. Selectivity for benzaldehyde increased from 76.9 to 87.6 % when catalyst amount increased from 5 to 10 mg, and then dropped to 76.6 % when catalyst amount increased to 20 mg due to formation of more by-products. Based on above results, 10 mg has been considered as optimum catalyst amount.

3.8 Reuse of the catalyst

After the reaction, the catalyst can be seen being adsorbed on the magnet. The catalyst together with the magnet can be easily separated by simple decantation after applying a magnetic field on the surface of the flask, and then subjected to the second run under the same conditions. The results are shown in Table 7. The selectivity for benzaldehyde changed slightly after five runs, but the conversion of styrene decreased from 16.5 to 12.4 %. The decrease in the activity could be mainly attributed to unavoidable loss of the catalyst during the process of collection. The results confirm that the nanocrystalline spinel **cat.4** has good stability and recyclable applicability for the oxidation of styrene with 30 % H_2O_2.

Table 7 Reuse of the catalyst

Recycle number	Conversion (%)	Selectivity (%)			
		BzA	PhAA	SO	Other
Fresh	16.5	85.8	4.2	6.0	4.0
1	15.7	87.6	4.8	5.1	2.5
2	14.6	83.9	5.2	5.4	5.5
3	13.3	85.7	4.9	5.7	3.7
4	12.9	86.1	4.6	4.9	4.4
5	12.4	87.1	5.0	4.9	3.0

Reaction conditions: styrene 17.4 mmol; **cat.4** 10 mg; H_2O 5.0 mL; temperature 80 °C; reaction time 6 h; styrene:H_2O_2 molar ratio 2:5

BzA benzaldehyde, *PhAA* phenylacetaldehyde, *SO* styrene oxide

4 Conclusions

Nanosized spinel-type Mg–Cu ferrite complex oxides were prepared by a simple and effective route of sol–gel auto-combustion using cheap precursors. The complex ferrite catalysts are more active and easily reusable catalysts for styrene oxidation in a green catalytic system and benzaldehyde is the main product. Protic solvent water is favorable for increasing the selectivity for benzaldehyde. The catalytic performances of the samples are highly related to their components and the $Mg_{0.5}Cu_{0.5}Fe_2O_4$ spinel has shown the highest catalytic activity. This work, along with other published ones, indicates that ferrite complex oxides have a considerable potential for becoming a kind of tunable catalysts in respect of catalytic performances and components. Based on this purpose, more efforts have been and will be focused on investigating structure-activity relationships of the ferrite complex oxides in catalytic oxidation reactions in our present and future work.

Acknowledgments The authors are grateful to the National Natural Science Foundation of China (51302222), the Scientific Research Fund of Northwest Normal University (NWNU-LKQN-10-28) and Program for Changjiang Scholars and Innovative Research Team in University (IRT1177) for financial support.

References

1. Yang Y, Ding H, Hao SJ, Zhang Y, Kan QB (2011) Appl Organomet Chem 25:262–269
2. Choudhary VR, Chaudhari PA, Narkhede VS (2003) Catal Commun 4:171–175
3. Ulmann's F (1985) Encyclopedia of industrial chemistry, 5th edn. VCH, Weinheim, p 469
4. Parihar S, Pathan S, Jadeja RN, Patel A, Gupta VK (2012) Inorg Chem 51:1152–1161
5. Samran B, Aungkutranont S, White TJ, Wongkasemjit S (2011) J Sol–Gel Sci Technol 57:221–228
6. Ahmad AL, Koohestani B, Bhatia S, Ooi SB (2012) Int J Appl Ceram Technol 9:588–598
7. Wang YR, Guo YJ, Wang GJ, Liu YW, Wang F (2011) J Sol–Gel Sci Technol 57:185–192
8. Tshentu ZR, Togo C, Walmsley RS (2010) J Mol Catal A 318:30–35
9. Sharma S, Sinha S, Chand S (2012) Ind Eng Chem Res 51:8806–8814
10. Barbero BP, Gamboa JA, Cadus LE (2006) Appl Catal B 65:21–30
11. Wang ZY, Fei WJ, Qian HC, Jin M, Shen H, Jin ML, Xu JY, Zhang WR, Bai Q (2012) J Sol–Gel Sci Technol 61:289–295
12. Faungnawakij K, Kikuchi R, Shimoda N, Fukunaga T, Eguchi K (2008) Angew Chem Int Ed 47:9314–9317
13. Kantam ML, Yadav J, Laha S, Srinivas P, Sreedhar B, Figueras F (2009) J Org Chem 74:4608–4611
14. Ma N, Yue YH, Hua WM, Gao Z (2003) Appl Catal A 251:39–47
15. Pardeshi SK, Pawar RY (2011) J Mol Catal A 334:35–43
16. Pardeshi SK, Pawar RY (2010) Mater Res Bull 45:609–615
17. Guin D, Barawati B, Manorama SV (2005) J Mol Catal A 242:26–31
18. Ramanathan R, Sugunan S (2007) Catal Commun 8:1521–1526
19. Zhang DH, Li HB, Li GD, Chen JS (2009) Dalton Trans 47:10527–10533
20. Shafi K, Gedanken A, Prozorov R, Balogh J (1998) Chem Mater 10:3445–3450
21. Srivastava DN, Perkas N, Gedanken A, Felner I (2002) J Phys Chem B 106:1878–1883
22. Ennas G, Marongiu G, Marras S, Piccaluga G (2004) J Nanopart Res 6:99–105
23. Manova E, Tsoncheva T, Paneva D, Mitov I, Tenchev K, Petrov L (2004) Appl Catal A 277:119–127
24. Ammar S, Helfen A, Jouini N, Fievet F, Rosenman I, Villain F, Molinie P, Danot M (2001) J Mater Chem 11:186–192
25. Hyeon T (2003) Chem Commun 8:927–934
26. Paike VV, Niphadkar PS, Bokade VV, Joshiw PN (2007) J Am Chem Soc 90:3009–3012
27. Chen LY, Shen YM, Bai JF (2009) Mater Lett 63:1099–1101
28. Cannas C, Falqui A, Musinu A, Peddis D, Piccaluga G (2006) J Nanopart Res 8:255–267
29. Zhang RJ, Huang JJ, Zhao HT, Sun ZQ, Wang Y (2007) Energy Fuels 21:2682–2687
30. Yue Z, Guo W, Zhou J, Gui Z, Li L (2004) J Magn Magn Mater 270:216–223
31. Tong JH, Bo LL, Li Z, Lei ZQ, Xia CG (2009) J Mol Catal A 307:58–63
32. Tong JH, Cai XD, Wang HY, Xia CG (2013) J Sol–Gel Sci Technol. doi:10.1007/s10971-013-3031-8
33. Cannas C, Falqui A, Musinu A, Peddis D, Piccaluga G (2006) J Nanopart Res 8:255–267
34. Silveira LB, Santos JG, Oliveira AC, Tedesco AC, Marchetti JM, Lima ECD, Morais PC (2004) J Magn Magn Mater 272:E1195–E1196
35. Chamritski I, Burns G (2005) J Phys Chem B 109:4965–4968
36. Yu T, Shen ZX, Shi Y, Ding J (2002) J Phys Condens Mat 14:613–618